NOAA Technical Memorandum ERL WPL-147

IMPROVEMENTS IN PROFILER WIND ESTIMATES USING SMOOTHED DATA IN THE SPECTRUM FINDER ALGORITHM

W. L. Eberhard

Wave Propagation Laboratory
Boulder, Colorado
June 1987

noaa NATIONAL OCEANIC AND ATMOSPHERIC ADMINISTRATION / Environmental Research Laboratories

NOAA Technical Memorandum ERL WPL-147

IMPROVEMENTS IN PROFILER WIND ESTIMATES USING SMOOTHED DATA IN THE SPECTRUM FINDER ALGORITHM

W. L. Eberhard

Wave Propagation Laboratory
Boulder, Colorado
June 1987

UNITED STATES
DEPARTMENT OF COMMERCE

Malcolm Baldrige,
Secretary

NATIONAL OCEANIC AND
ATMOSPHERIC ADMINISTRATION

Anthony J. Calio,
Administrator

Environmental Research
Laboratories

Vernon E. Derr,
Director

NOTICE

Mention of a commercial company or product does not constitute an endorsement by NOAA Environmental Research Laboratories. Use for publicity or advertising purposes of information from this publication concerning proprietary products or the tests of such products is not authorized.

For sale by the National Technical Information Service, 5285 Port Royal Road
Springfield, VA 22161

CONTENTS

		Page
ABSTRACT		1
1.	INTRODUCTION	1
2.	METHOD	2
3.	FINDER ALGORITHMS	4
4.	RESULTS OF SIMULATIONS	6
	4.1 Behavior of Smoothers for Base Case	7
	4.2 Sensitivity to Spectrum Shape	10
	4.3 Sensitivity to Spectrum Width $\langle\sigma\rangle$	12
	4.4 Sensitivity to Number of Spectral Points K	16
	4.5 Sensitivity to Number of Averaged Spectra L	18
5.	IMPROVEMENT IN WEAK SIGNAL DETECTION	20
6.	IMPROVEMENTS ON A CONSENSUS AVERAGE	22
7.	SUMMARY	24
8.	REFERENCES	25

IMPROVEMENTS IN PROFILER WIND ESTIMATES USING SMOOTHED DATA IN THE SPECTRUM FINDER ALGORITHM

W. L. Eberhard

ABSTRACT. Wind profilers obtain the component of wind velocity parallel to the radar beam by calculating the first moment of the Doppler spectrum. An effective data processing algorithm uses peak detection to locate the subset of the spectrum containing the Doppler signal before the mean frequency is calculated. Simulations showed that smoothing the data before finding the peak yields better accuracy when the signal-to-noise ratio is marginal. Sensitivity studies considered the dependence of the improvement on signal shape, smoother shape, number of spectral points, width of the signal spectrum, and number of spectra in the average, all as a function of signal-to-noise ratio. The effect of the smoother can also be interpreted as improved sensitivity with no loss of accuracy when signal-to-noise ratio is low. Simulations of consensus averaging demonstrated that the smoothed finder improves both the accuracy and effective sensitivity.

1. INTRODUCTION

The processing algorithms for wind profiler data determine the mean Doppler frequency of the signal spectrum in the presence of noise. The Colorado wind-profiling network (Strauch et al., 1984b) and the planned NOAA 30-station demonstration network (Chadwick and Hassel, 1987) both use peak detection to find the approximate position of the signal in the measured spectrum. The algorithms next calculate the power-weighted mean frequency over a range of contiguous spectral points that exceed the noise level and that include the peak. This simple method performs very well when the signal-to-noise ratio (SNR) is high. However, as the SNR degrades, the algorithm increasingly finds a large, random noise spike that can be far removed from the signal spectrum. This can cause large errors in the mean frequency estimate. Consensus averaging (Strauch et al., 1984b) removes many, but not all, of the obvious errors in the hour-average wind estimate.

This study investigates the advantages of a finder algorithm that applies a smoother or running filter to the spectrum before using the peak criteria. The other steps in data processing use the unfiltered spectrum and are identical to those performed with the peak finder algorithm. The smoother should diminish

the influence of the occasionally large noise spike and lead to better wind estimates when the SNR is poor.

2. METHOD

The effectiveness of the finder algorithms was investigated by applying them to spectra of signal plus noise simulated by computer. The interactive effects of the other processing steps, such as defining the range of contiguous spectral points for the mean frequency calculation, are easily included. (The computer programs will also be used in a later study of other aspects of the data processing, such as the effect of the noise threshold on the estimated spectral width.)

Power density spectra were simulated by the method of Zrnic (1975). The profilers obtain a complex time series of the signal and perform a discrete Fourier transform. The magnitudes of the Fourier coefficients are squared to obtain the spectrum. Since the signal echo is generated by scatterers that are randomly positioned, the signal power density S(i) varies randomly between spectral points, which are denoted by the index i. The noise power N(i) is also generated randomly. The probability distribution of the spectral density

$$P(i) = S(i) + N(i)$$

is exponential, with standard deviation equal to the expected value. Following Zrnic (1975), we used a computer's random number generator to simulate the stochastic nature of P(i) while avoiding the more computer-intensive task of simulating the complex time series.

The profile of the expected signal spectrum <S(i)> in most of the simulations had the Gaussian shape

$$\langle S(i) \rangle = \frac{\langle S_T \rangle}{(2\pi)^{1/2} \langle \sigma \rangle} \exp\left[\frac{(i - \langle F \rangle)^2}{2\langle \sigma \rangle^2}\right] ,$$

where <F> is the expected value of the mean frequency and $\langle S_T \rangle$ is the expected value of the total signal power. Frequencies in this study are nondimensional

and are expressed in terms of spectral point number. The peak was near the center of the profiler spectrum (i.e., zero velocity) to avoid the complications of aliasing. A few simulations were also performed with a signal spectrum of rectangular shape, given by

$$\langle S(i) \rangle = \frac{\langle S_T \rangle}{(12)^{1/2} \langle \sigma \rangle}$$

if

$$(i - \langle F \rangle)^2 < \langle \sigma \rangle^2$$

and zero, otherwise.

The expected value of the noise had constant spectral density, i.e., $\langle N(i) \rangle = \langle N \rangle$. The expected SNR was defined as the ratio of the total power in the expected Doppler spectrum to the total expected noise power, or

$$\langle SNR \rangle = \frac{\sum_{i=1}^{K} \langle S(i) \rangle}{K \langle N \rangle} ,$$

where K is the number of points in the spectrum.

The profilers average several tens of spectra to improve the effective SNR. The simulations likewise averaged L independent spectra.

The method (Hildebrand and Sekhon, 1974) to estimate the noise level of the averaged spectrum during the simulations was identical to that used by the profilers. The finder algorithm was applied next, followed by calculation of the mean frequency estimate F of the averaged spectrum.

Since the spectra are random, F also varies about $\langle F \rangle$. The simulations to compare the finder algorithms were therefore performed numerous times to obtain the statistics of these variations. Independent cases numbering C = 400 for each set of parameters cut an adequate compromise between large C for approaching the ensemble average and small C to limit the computer resources required. The standard deviation of F, denoted by σ_F, for the 400 cases gave a

satisfactory and succinct measure of the performance of the finder algorithms. The average of F ($\bar{F}$) deviated from <F> by an insignificant amount for the current purpose. In other words,

$$\sigma_F >> |\bar{F} - \langle F \rangle|$$

for C = 400.

3. FINDER ALGORITHMS

Four finder algorithms were studied.

(1) Peak or d = 1.

The first method was the peak finder currently in use on the profilers. The other methods reduce to this when the domain d of the smoother is unity.

(2) Rectangular smoother, peak subsearch.

The second method began simply with a centered running sum over an odd number d of spectral points. Values of the standard deviation σ_s of the smoother function are listed in Table 1. As d becomes large, σ_s approaches $d/(12)^{1/2}$. The filter wrapped around the spectrum whenever it extended beyond the edges. For instance, for d = 5, the data point of the smoothed spectrum at i = 2 was the sum from the unfiltered spectrum of P(i) at i = K, 1, 2, 3, and 4. The location i_p of the peak in the filtered spectrum was found next. A subsearch was then performed to ensure that power in the unfiltered spectrum at the found location i_f had power greater than the noise level. The i_f was set at the location of the peak P(i) in the unfiltered spectrum within the range $i_p-(d-1)/2 \leq i \leq i_p+(d-1)/2$, except that the subsearch did not wrap around the spectrum.

(3) Rectangular smoother, nearest positive subsearch.

The third method was identical to the second, except for the subsearch. After i_p was found from the smoothed spectrum, i_f was set at i_p if the power at i_p in the unfiltered spectrum exceeded the noise level. If not, the bracketing pair of points were examined. If the power in at least one of them exceeded the noise level, the location with the larger power was selected as i_f. If necessary, further bracketing pairs were examined in turn. This subsearch also did not wrap around the ends of the spectrum.

Table 1. Standard deviation (σ_s) of smoother function

	Rectangular		Cosine-squared	
d	Exact	$d/\sqrt{12}$	Exact	$d(1/12 - 1/2\pi^2)^{1/2}$
1	0	0.289	0	0.181
3	0.816	0.866	0.250	0.542
5	1.414	1.443	1.080	0.904
7	2.000	2.021	1.444	1.265
9	2.582	2.598	1.807	1.627
11	3.162	3.175	2.169	1.988

(4) Cosine-squared smoother, nearest positive subsearch.

The fourth method used a weighted smoother with a bell shape for the running sum. The smoother was

$$P(i_s) = \sum_{i=i_s-(d-1)/2}^{i_s+(d-1)/2} \{P(i) \cos^2[\pi(i - i_s)/(d + 1)]\} ,$$

where i_s is the data point in the smoothed spectrum. Exactly like the last few steps of Method 3, the peak was located in the smoothed spectrum, and i_f was set at the closest point to i_p in the unfiltered spectrum where P(i) > N. Table 2 lists the standard deviation of the function and the theoretical expression valid in the limit of large d.

The finder algorithms are listed in order of complexity, the peak method being the simplest. However, Method 4 is still easy to implement. The analysis below shows that the algorithms are listed in reverse order of performance. Sensitivity studies used the cosine-squared method, because it gave the best results overall.

Table 2. Effective gain (dB) in weak signal detectivity

$\langle\sigma\rangle$	K	L	Spectrum shape	Smoother shape	σ_F		
					K/13.8	K/32	$\langle\sigma\rangle$
4	64	16	Gaussian	Rectangular	2.0	2.6	2.1
4	64	16	Gaussian	Cosine²	2.1	3.2	2.1
3.75	64	16	Rectangular	Rectangular	2.4	2.7	2.3
3.75	64	16	Rectangular	Cosine²	2.3	3.0	2.2
1	64	16	Gaussian	Cosine²	0.9	1.3	1.1
2	64	16	Gaussian	Cosine²	1.9	2.4	2.4
8	64	16	Gaussian	Cosine²	2.4	0.4	2.6
4	32	16	Gaussian	Cosine²	2.3	0.4	2.6
4	128	16	Gaussian	Cosine²	3.0	3.1	3.2
4	256	16	Gaussian	Cosine²	2.4	3.3	3.1
4	64	4	Gaussian	Cosine²	1.8	2.5	1.9
4	64	8	Gaussian	Cosine²	2.6	2.6	2.2
4	64	32	Gaussian	Cosine²	2.3	2.5	2.7
4	64	64	Gaussian	Cosine²	4.2	2.9	2.9

4. RESULTS OF SIMULATIONS

A baseline set of spectral parameters was selected to examine the effect of the finder algorithms on σ_F. The baseline parameters are Gaussian spectrum with $\langle\sigma\rangle$ = 4, K = 64, <F> = 32, L = 16, and C = 400. These are typical of the Colorado network at the maximum of the jet stream, where <SNR> is often small. After determining the general behavior of the finder algorithms for this situation, sensitivity studies were performed by changing the shape of the signal spectrum, $\langle\sigma\rangle$, K, or L. The <SNR> for the base case ranged from -16 to -4 dB in steps of 1 dB. The sensitivity studies also used 1 dB steps in <SNR>, although sometimes over a different range. The simulations highlighted the effect of the smoothers for each combination of spectral parameters by applying them to the identical set of averaged spectra. However, the set of spectra are independent for different values of <SNR>, which provides an indication of the statistical variability of σ_F in the simulations.

4.1 Behavior of Smoothers for Base Case

The results for Methods 1 and 3 appear in Fig. 1. For <SNR> ≥ -6 dB the magnitude of σ_F is identical for all values of d. The signal spectrum is sufficiently above the noise that smoothing yields no improvement. Even so, the accuracy in F, as inferred from the increase in σ_F, diminishes as <SNR> decreases from -4 to -6 dB. A change in the slope of the curve for d = 1 at about <SNR> = -7.5 marks the point where noise spikes begin to interfere with locating the approximate position of the signal spectrum. As <SNR> declines further, σ_F increases quite rapidly for d = 1. The slope becomes less severe for <SNR> < -12 dB and asymptotically approaches the no-signal limit of $64/\sqrt{12} = 18.5$.

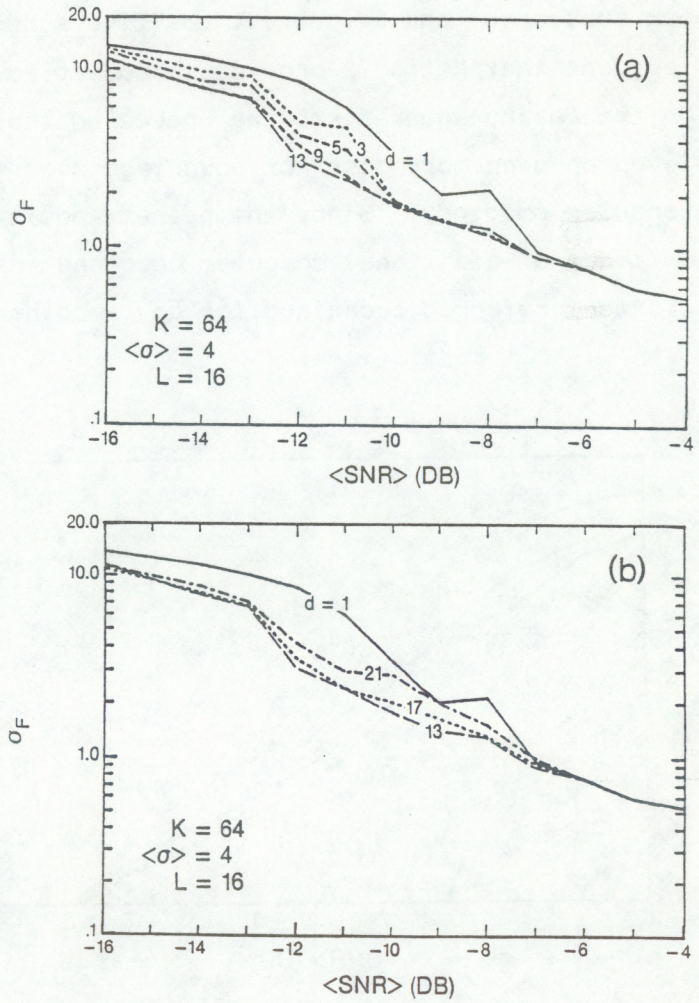

Figure 1. σ_F from Methods 1 (peak) and 3 (rectangular smoother with nearest positive subsearch) on a Gaussian-shaped spectrum. (a) d ≤ 13; (b) d ≥ 13 and d = 1.

The rectangular smoother shifts the position of the break in the slope to lower values of <SNR>. The strong contamination by the noise spikes begins at about -10 and -12 dB for d = 3 and 13, respectively. The improvement in σ_F is smaller for <SNR> $\leq$ -13 dB. The transition from peak finder to d = 3 yields considerable improvement. Further increments in d provide additional advantage up to the best case of d = 13. The performance of the smoother degrades somewhat as d increases beyond 13. The value of σ_s for the d = 13 smoother is 3.75, which is close to $\langle\sigma\rangle$ of the simulated signal spectrum. The best smoother gives σ_F approximately a factor of 2.5 smaller than the peak finder for -8 dB $\leq$ <SNR> $\leq$ -12 dB. Over this same range of <SNR>, the d = 13 finder is able to achieve the same σ_F for <SNR> roughly 2 dB smaller than the peak finder.

Methods 2 (peak subsearch) and 3 (nearest positive subsearch) are compared in Fig. 2. It is evident that Method 3 provides a modest advantage over Method 2. A brief test on the cosine-squared smoother revealed that the nearest positive subsearch enjoyed an even more distinct advantage over the peak subsearch than with the rectangular smoother. Since the nearest positive subsearch requires only a few lines of additional computer code and insignificant computation time, it is the preferred technique for any smoother function.

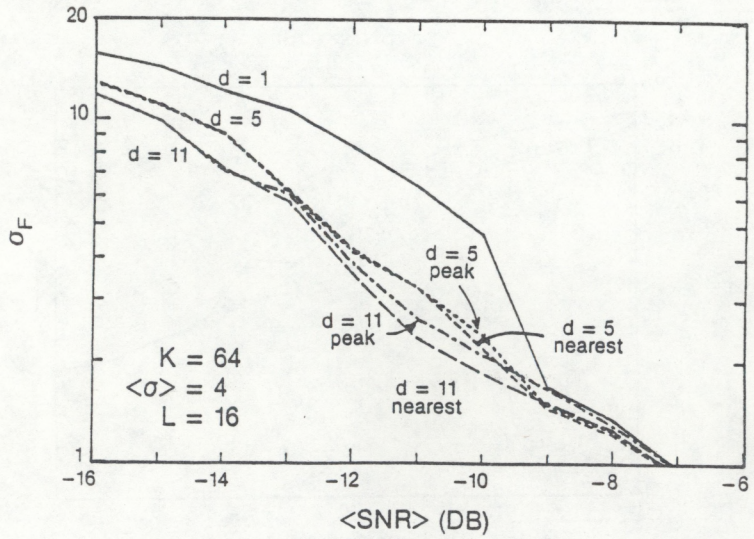

Figure 2. σ_F from Methods 1, 2 (rectangular smoother with peak subsearch), and 3 on a Gaussian-shaped spectrum.

The behavior of Method 4 for the base case is shown in Fig. 3. The spectra are the same as in Fig. 1. The value of d was incremented by 2 from 1 through 17 and then by 4 from 17 to 49. This smoother improves the accuracy of F in a manner very similar to Method 3, except that d = 21 yielded the smallest overall σ_F. (It is possible that d = 23 would be slightly better.) The approximate standard deviation of the smoother function, calculated from the analytical form for large d, is 3.80 for d = 21. This again closely matches the standard deviation of the signal spectrum. The σ_F grows as d increases above the best value, but the degradation is less rapid than in Method 3 in the critical region of <SNR> ~ -9 dB. Method 4 with d = 21 also shows slightly smaller σ_F overall than Method 3 with d = 13. This fact, combined with the better stability shown by Method 4 when the smoother is wider than the spectrum, may well justify the

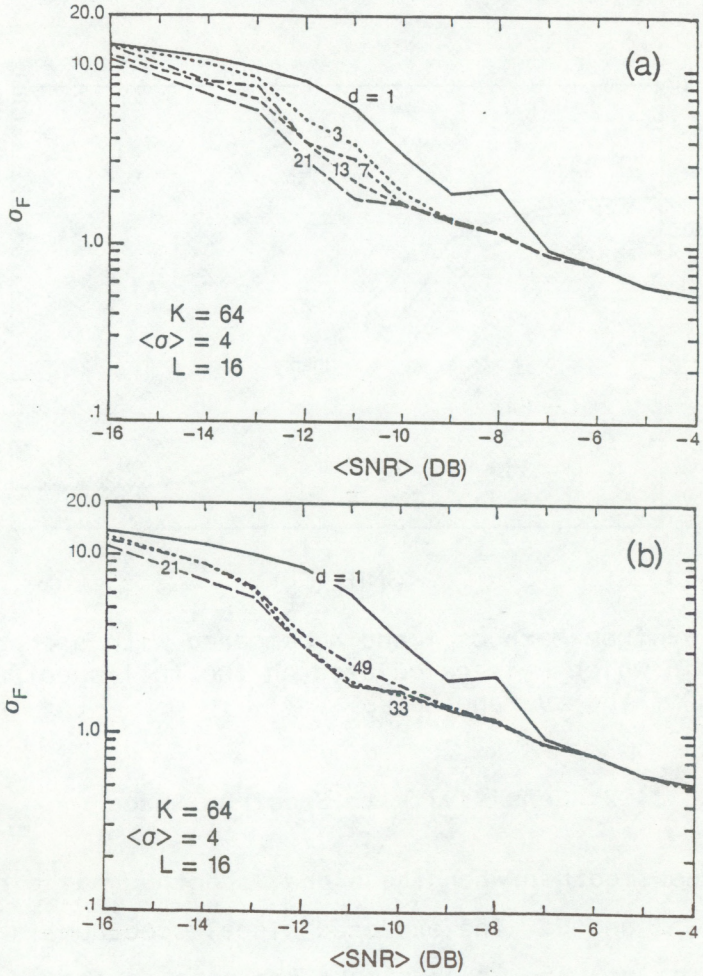

Figure 3. σ_F from Method 4 (cosine-squared smoother with nearest positive subsearch) on a Gaussian-shaped spectrum. (a) d ⩽ 21; (b) d = ⩾ 21 and d = 1.

complexity of the weighting functions in Method 4 compared with the simple running average of Method 3.

The performance of Methods 1 and 4 are compared over the range of -20 dB ≤ <SNR> ≤ 30 dB at 2 dB increments in Fig. 4. A theoretical prediction, based on Berger and Groginsky (1973) but modified here for L spectra averaged together, is also shown. The prediction is for F calculated as the first moment of the entire spectrum after the expected value of the noise has been subtracted. All three agree closely for high <SNR>. The peak finder with the first moment calculated on the contiguous range of spectral values that exceed the noise level provides a significant advantage over the full spectrum method for -10 dB ≤ <SNR> ≤ 5 dB. The theoretical treatment becomes invalid as <SNR> declines below -10 dB. The smoother achieves additional improvement for -15 dB ≤ <SNR> ≤ -11 dB.

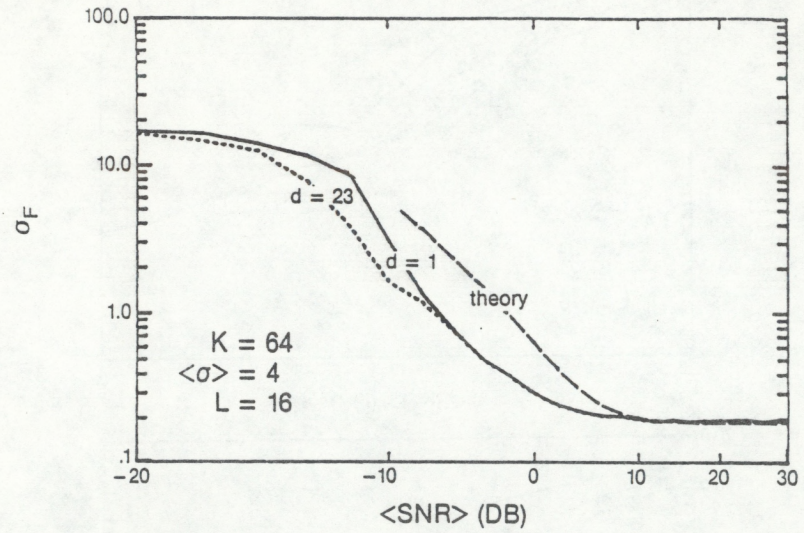

Figure 4. σ_F from Methods 1 and 4 compared with a theoretical prediction in which F is calculated on the full spectrum after subtraction of the average noise.

4.2 Sensitivity to Spectrum Shape

The effect of the smoother when the signal spectrum has a rectangular shape is evaluated in Figs. 5 and 6. The expected signal spectrum is nonzero at 13 data points, giving $\langle\sigma\rangle = 3.75$, which almost the same as the $\langle\sigma\rangle$ for the Gaussian base case. The rectangular smoother performs best (Fig. 5) when it matches the spectrum with d = 13. The improvement is similar to that with the

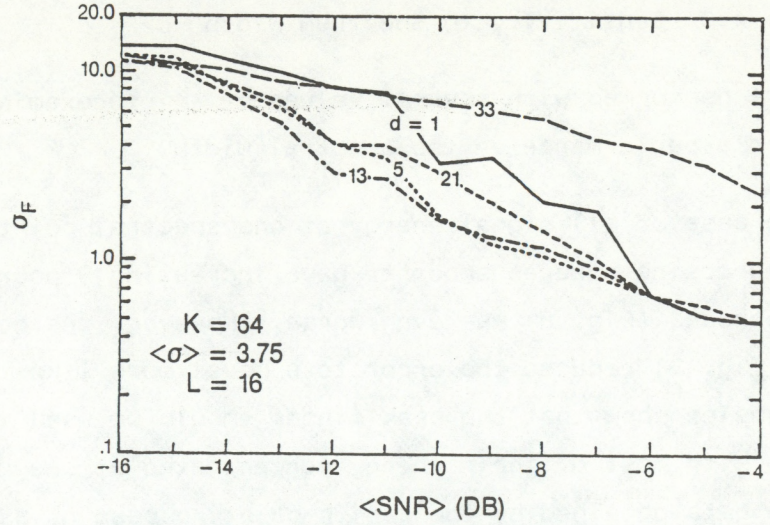

Figure 5. σ_F from Methods 1 and 3 on a rectangular-shaped spectrum.

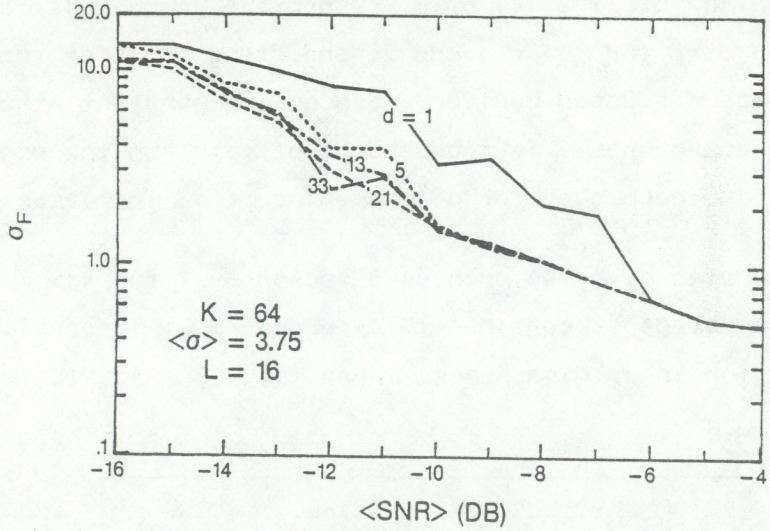

Figure 6. σ_F from Methods 1 and 4 on a rectangular-shaped spectrum.

base case. An excessively wide smoother (d = 33) gives much poorer results than even the peak finder. Fig. 6 shows the results for the cosine-squared filter, which first reaches best performance when d = 23 or σ_s = 3.8. This smoother's results were almost identical with those of the rectangular smoother when d = 13 and even slightly better at <SNR> = -11 dB. Thus, the shape of the smoother in relation to the shape of the spectrum is of secondary importance. However, the cosine-squared smoother is more stable when $\sigma_s > \langle\sigma\rangle$.

4.3 Sensitivity to Spectrum Width <σ>

Simulations were performed with several values of <σ> to examine the dependence of the smoother's performance on the spectral width.

For the extreme case of all signal energy at one spectral point (<σ> = 0), Fig. 7 shows that the cosine-squared smoother gave increasingly poor results as d became larger. Method 3 (Fig. 8) was even worse. However, the peak subsearch of Method 2 (Fig. 9) reduced the error to a level more like that of Method 4. These examples show that the peak finder should be used if spectra are extremely narrow with most of their energy concentrated at one data point. This often occurs in data obtained by the zenith-pointing beam of a VHF radar.

Figures 10-13 consider the application of a cosine-squared smoother to Gaussian spectra with <σ> of 1, 2, 4, or 8, respectively. Simulations were performed for steps in d of 2 for <σ> = 1 and 2, and steps of 4 for <σ> = 8. The base case (<σ> = 4) was discussed earlier. Since K is constant, the limiting value of σ_F as <SNR> approaches 0 is independent of <σ>. On the right side of the graphs, where σ_F is independent of d, the value of σ_F increases with <σ>.

The smoother improves σ_F by as much as a factor of 7 for <σ> = 1 in Fig. 10, but this large advantage is confined to a narrow <SNR> interval. As <σ> increases, the reduction in σ_F disappears. When <σ> = 8 (Fig. 13) the best

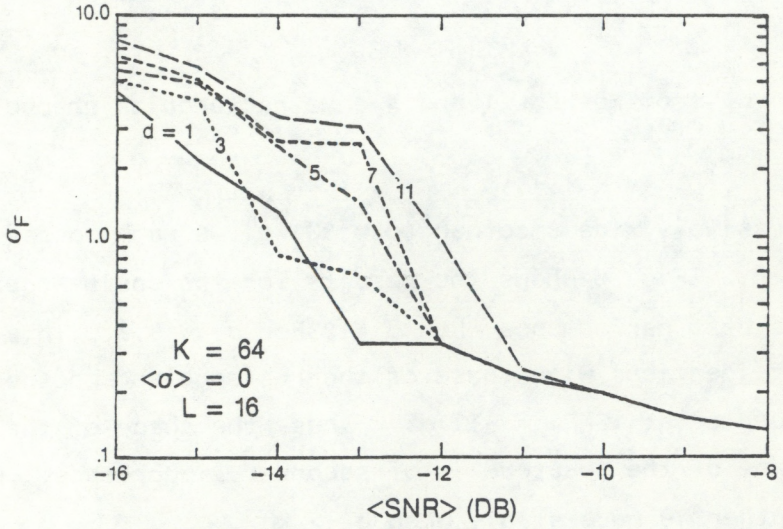

Figure 7. σ_F from Methods 1 and 4 on a single-peak spectrum.

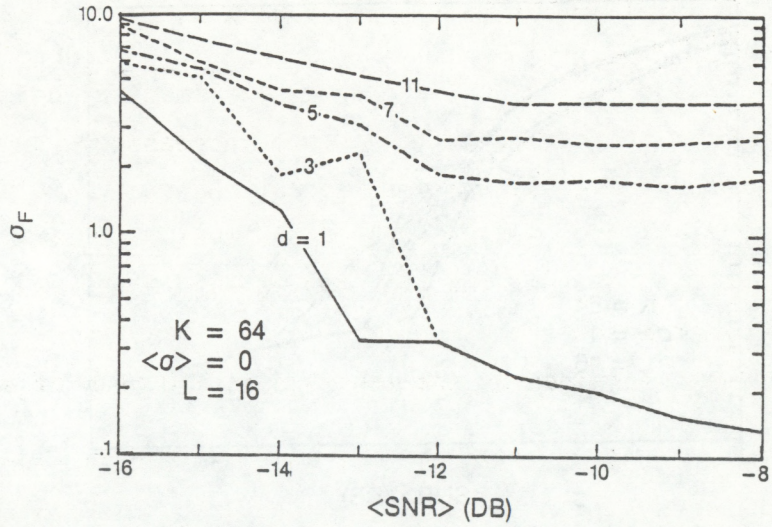

Figure 8. σ_F from Methods 1 and 3 on a single-peak spectrum.

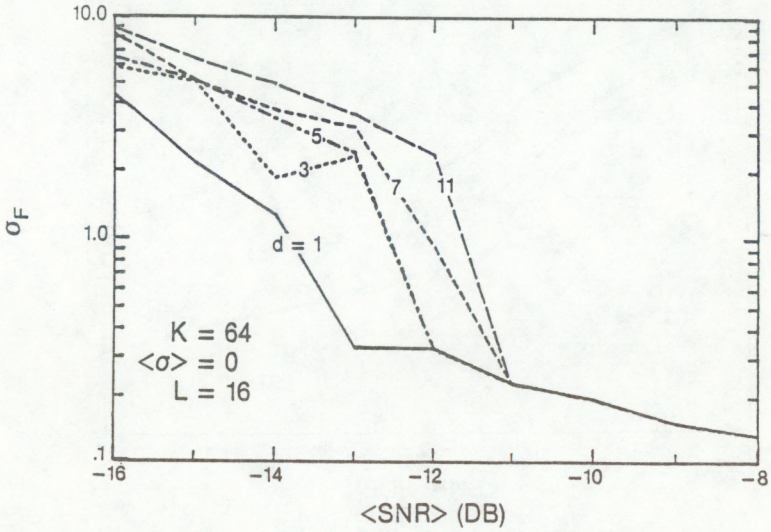

Figure 9. σ_F from Methods 1 and 2 on a single-peak spectrum.

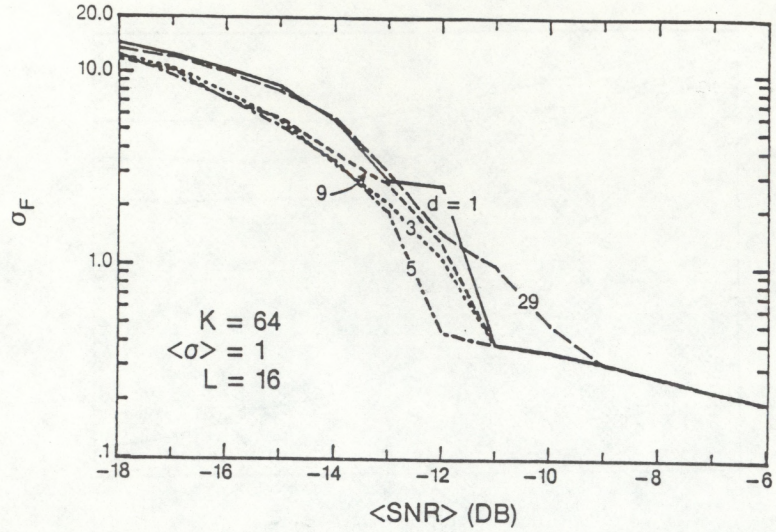

Figure 10. σ_F from Method 4 on a Gaussian-shaped spectrum with $\langle\sigma\rangle = 1$.

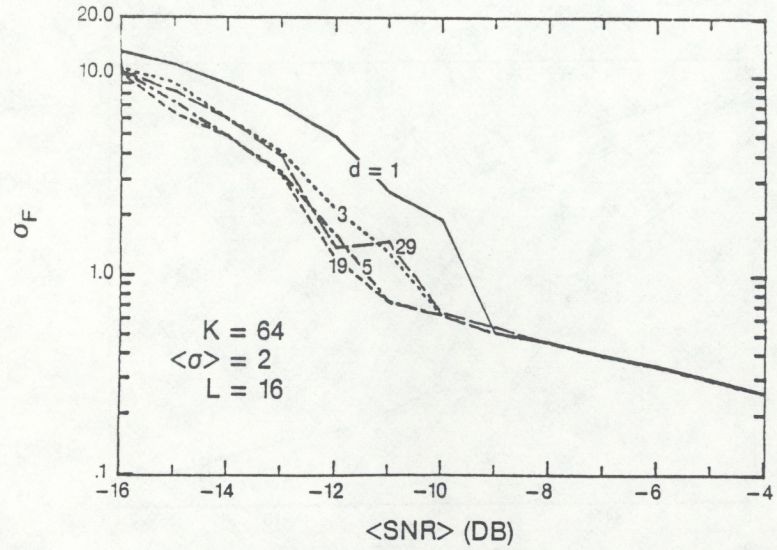

Figure 11. σ_F from Method 4 on a Gaussian-shaped spectrum with $\langle\sigma\rangle = 2$.

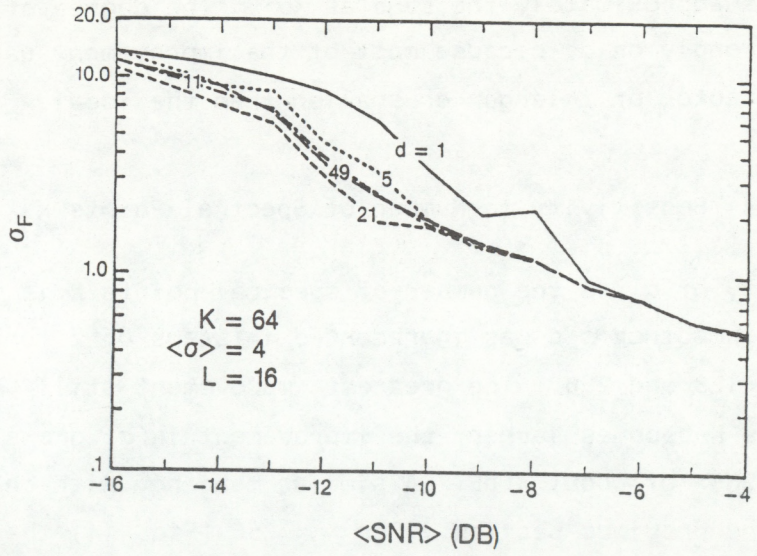

Figure 12. σ_F from Method 4 on a Gaussian-shaped spectrum with $\langle\sigma\rangle = 4$, K = 64, and L = 16. This is the base case for the sensitivity studies.

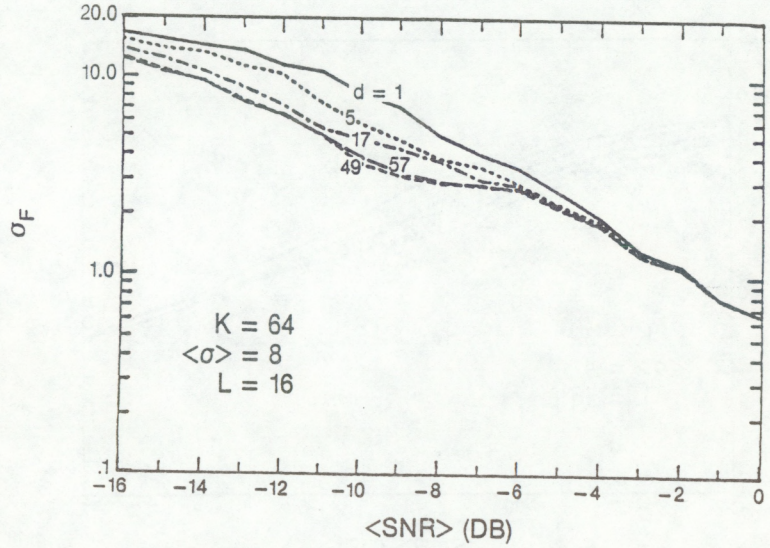

Figure 13. σ_F from Method 4 on a Gaussian-shaped spectrum with $\langle\sigma\rangle = 8$.

smoother reduces σ_F by a factor of about 2.5 over a range of <SNR> where σ_F remains quite large, even for the optimum d. The smoother yields the best results when σ_s is approximately the same as $\langle\sigma\rangle$. The degree of optimization does not depend strongly on d, because most of the improvement usually remains even when σ_s is a factor of 2 larger or smaller than the ideal.

4.4 Sensitivity to Number of Spectral Points K

The sensitivity of σ_F to the number of spectral points K is treated in Figs. 14-16 and 12. The smoother's d was incremented in steps of 2 for K = 32, and in steps of 4 for K = 128 and 256. The greatest improvement still occurs when σ_s matches $\langle\sigma\rangle$. As K becomes larger, the improvement in σ_F grows, especially within a band in <SNR> of about 4 dB. A similar tendency with changes in $\langle\sigma\rangle$/K was also seen in the previous section. For K = 256 (Fig. 14) the best improvement between d = 1 and 29 exceeds an order of magnitude; for K = 32 it reaches no more than a factor of about 2.5. Note that $\sigma_F \approx 1$ where the smoother first makes a difference, independent of K. However, the asymptotic limit of σ_F for <SNR> = 0 is proportional to K. The effect of the smoother in the transition region between these situations is therefore more dramatic for large K.

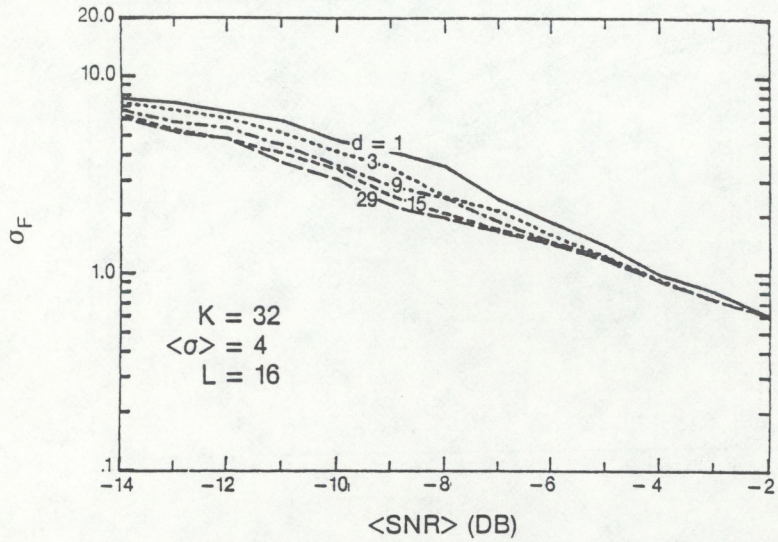

Figure 14. σ_F from Method 4 on a Gaussian-shaped spectrum with K = 32.

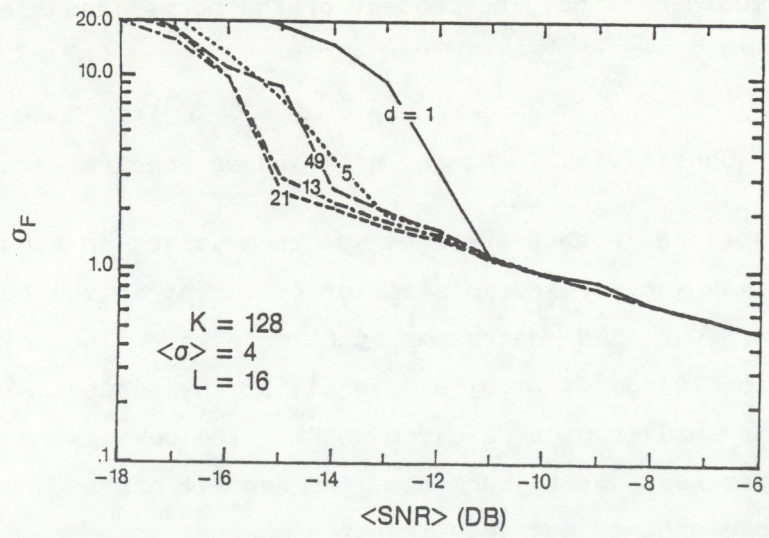

Figure 15. σ_F from Method 4 on a Gaussian-shaped spectrum with K = 128.

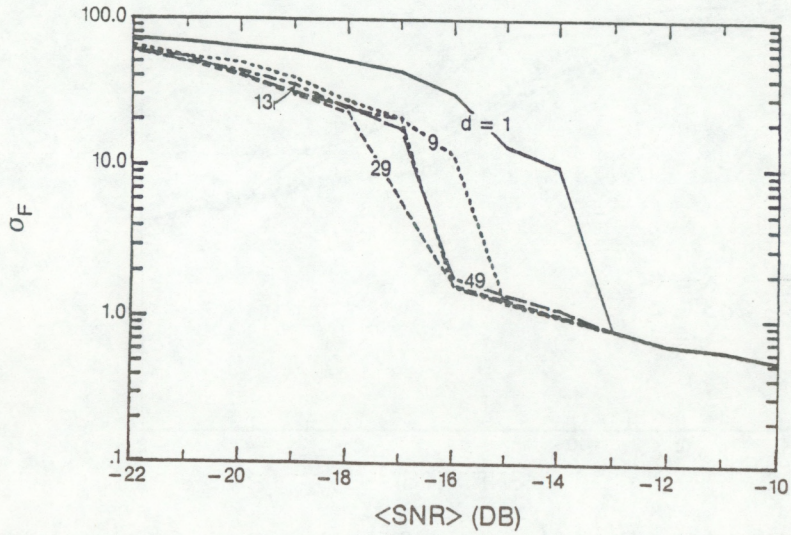

Figure 16. σ_F from Method 4 on a Gaussian-shaped spectrum with K = 256.

We can also compare Fig. 15 and 11, which both have $\langle\sigma\rangle/K = 1/8$. The smoothers yield substantially more improvement in the case of larger K; i.e., the effect of the smoother is not independent of the normalized spectral width $\langle\sigma\rangle/K$.

4.5 Sensitivity to Number of Averaged Spectra L

The number of spectra in each averaged spectrum varies in Figs. 17-20 and 12. The value of d was incremented in steps of 4, except in the base case. The magnitude of σ_F at a given <SNR> decreases as L increases. The point where the curves of σ_F begin to diverge is at $\sigma_F \cong 1$ in all of these cases. However, the increase in L creates smaller σ_F at a given <SNR>. The best improvement still occurs when σ_s matches $\langle\sigma\rangle$. As L increases, the benefit of the smoothers increases a noticeable amount, but less than the changes in benefit seen with changes in $\langle\sigma\rangle$ or K.

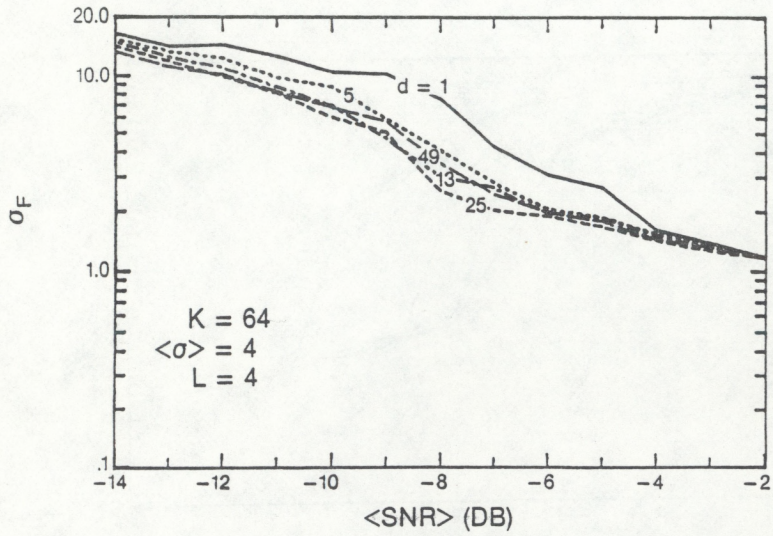

Figure 17. σ_F from Method 4 on a Gaussian-shaped spectrum with L = 4.

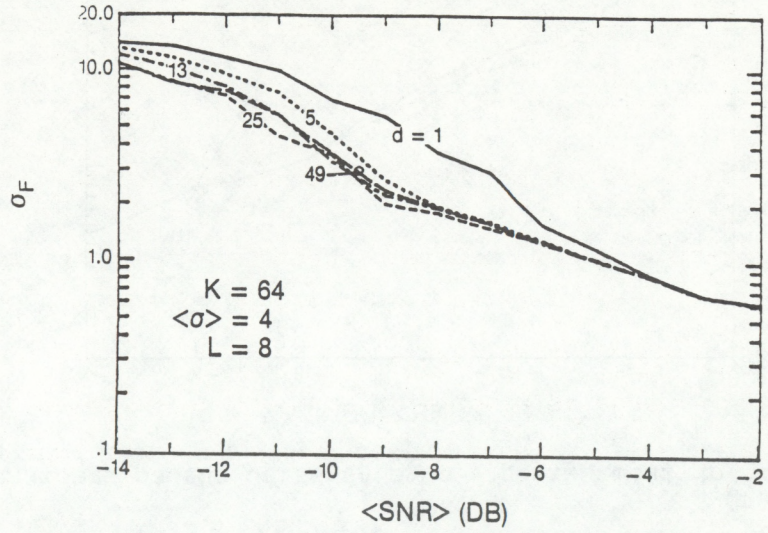

Figure 18. σ_F from Method 4 on a Gaussian-shaped spectrum with L = 8.

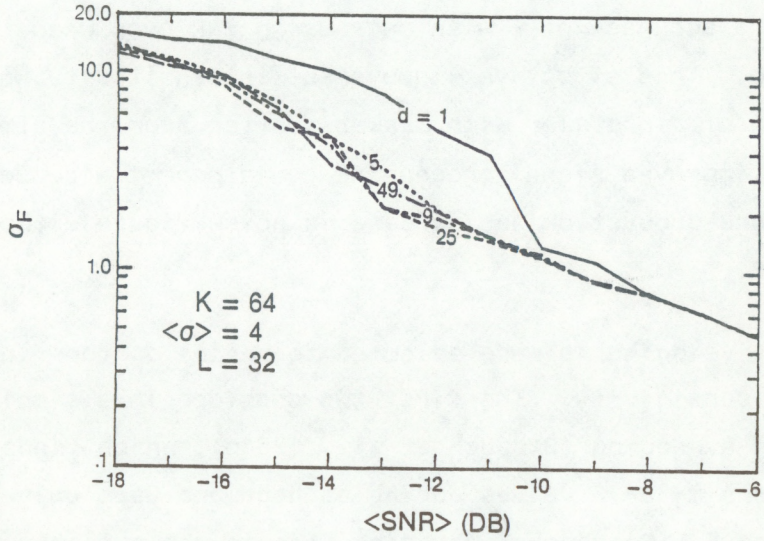

Figure 19. σ_F from Method 4 on a Gaussian-shaped spectrum with L = 32.

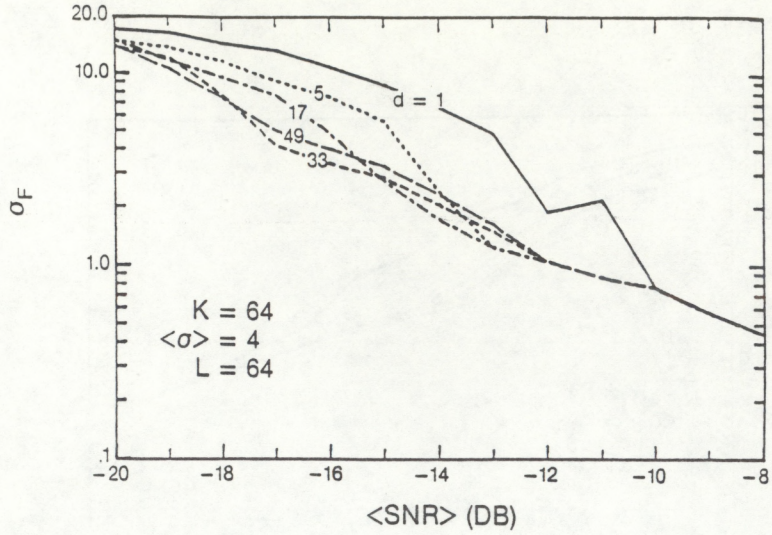

Figure 20. σ_F from Method 4 on a Gaussian-shaped spectrum with L = 64.

5. IMPROVEMENT IN WEAK SIGNAL DETECTION

The improvement accomplished by a smoothed finder was interpreted in Sec. 4 as better accuracy in F as quantified by a decrease in σ_F at a particular <SNR>. The effect of the smoother can also be viewed as the change in <SNR> at a particular σ_F, which can be interpreted as an increase in effective sensitivity of the profiler with no loss of accuracy in F. This latter interpretation expresses the greater ability of the smoothed finder to recognize the Doppler signal in the presence of considerable noise. It also accounts for the competing decline in the accuracy of F with decreasing SNR even when the signal is successfully located. This effective improvement in sensitivity would allow successful operation of a profiler with weaker scatter from the atmosphere. On the other hand, the improved signal processing could permit a reduction in the radar's power-aperture product or an increase in noise figure without compromising accuracy in F.

Three illustrative criteria were selected to define σ_F for finding the effective change in sensitivity. The first two consider in a simple way the concept of consensus averaging (Strauch et al., 1984b), which finds the most prominent cluster of similar F values during an hour and uses only these to compute the hour-average F. Consensus averaging rejects the outliers that occur when SNR is too low. Setting the cluster span at χ = K/16 and requiring at

least 4 out of 12 values of F to fall within this span has proved very successful for K = 64.

(1) The first criterion for σ_F is that, on average, no more than 2/3 of the F values fall outside <F> ± $\chi/2$. If we assume that F for a given set of parameters K, L, and <σ> is normally distributed, then

$$\sigma_F = \chi/(2 \times 0.43)$$

is the limit. This version gives the largest σ_F that can be considered reasonable.

(2) The second criterion requires that at least 68% of the F values fall within a consensus span centered on <F>, or

$$\sigma_F = \chi/2,$$

where F is again assumed to be normally distributed. A distinct majority of the F estimates will meet the consensus, and good accuracy can be expected in the hour-average F.

(3) The third limit uses the width of the Doppler spectrum as a criterion and requires

$$\sigma_F = \langle\sigma\rangle.$$

The results are listed in Table 2 for a variety of spectral parameters selected from the base case and sensitivity studies. The peak finder is compared with the smoother that performed the best for the particular circumstances. The difference in <SNR> for satisfactory performance varies from one situation to another (partly because of the random character of the simulations), but an effective gain of slightly more than 2 dB is typical.

6. IMPROVEMENTS ON A CONSENSUS AVERAGE

Simulations were also required to understand the combined effects of a smoothed finder and the consensus average, because both procedures are quite nonlinear. The baseline set of parameters defined the averaged spectra, from which individual estimates of F were calculated as in Sec. 4.1. The finders used d = 1 and also cosine squared with d = 5, 21, and 49. Simulations were carried out at 1 dB steps in <SNR>, with the four finders operating on the same set of spectra at a given <SNR>.

The Colorado network, which finds the consensus average [F] from 12 values of F spanning one hour of measurements, was the pattern for the simulations. The consensus average procedure first finds the cluster of data points with the maximum number n of F values that fall within a range of 4 spectral points of each other. [F] was the average of these n values of F when $n \geq 4$, but [F] remained undefined if $n \leq 3$. The computer simulated the consensus average 500 times for ecah data point in Figs. 21-23.

The smoothers find larger clusters than when d = 1 (Fig. 21), with the matched smoother at d = 21 performing noticeably better than d = 5 or 49. The mean number n for the various finders converge to 12 as <SNR> increases above -8 dB. The smoothers at low <SNR> seem to be converging approximately to n = 2.7, which is the mean cluster size from the simulations of Strauch et al. (1984a) for <SNR> = 0. The data in Fig. 22 show that the smoothed finders generate more clusters that meet the $n \geq 4$ consensus criterion than the peak finder, especially for $-20 \text{ dB} \leq \langle SNR \rangle \leq -14 \text{ dB}$. Over this range, the d = 21 smoother obtains as many cases with $n \geq 4$ as the peak finder does at about 3 dB higher <SNR>. Also, at a particular <SNR>, the number of cases with $n \geq 4$ is 30-100% larger at d = 21 than at d = 1. Therefore, when the SNR is marginal, the smoothed finders enable the consensus procedure to determine an adequate cluster and calculate [F] significantly more often than when d = 1.

Not only do the smoothers give more frequent success in the consensus average, but the accuracy in [F] also improves significantly for d = 21 and 49 (Fig. 23). The overall accuracy in [F] for d = 5 increased only slightly in this simulation. The band of <SNR> where the smoothers appreciably change the accuracy of [F] in Fig. 23 is lower in <SNR> than the band in Fig. 3 for the individual values of F.

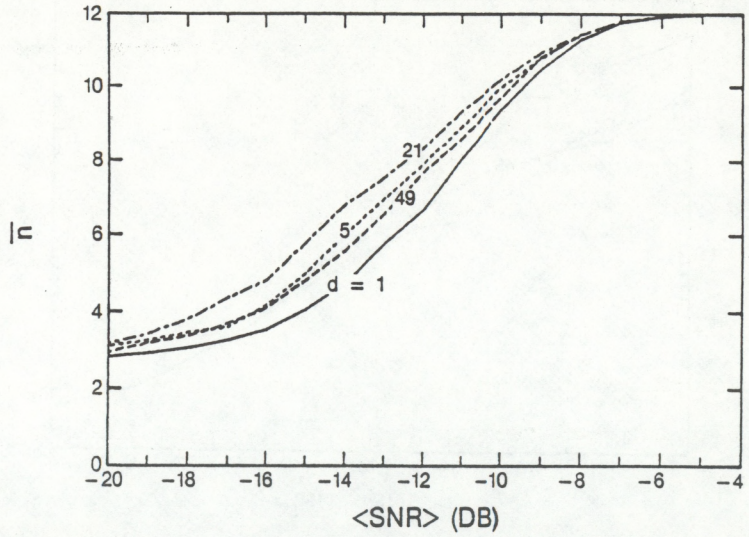

Figure 21. Mean n of largest cluster found by the consensus procedure as a function of <SNR>. See text for parameters in the simulation.

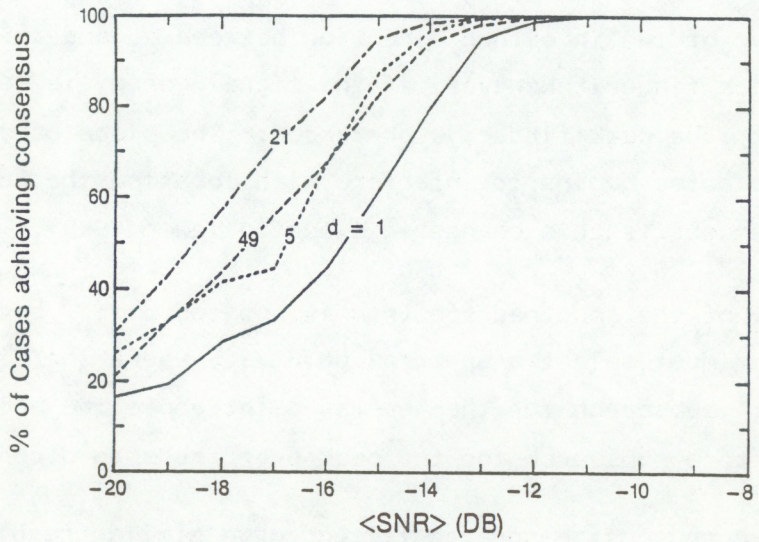

Figure 22. Percents of cases meeting the consensus criterion $n \geq 4$ versus <SNR> for the same simulations as in Fig. 21.

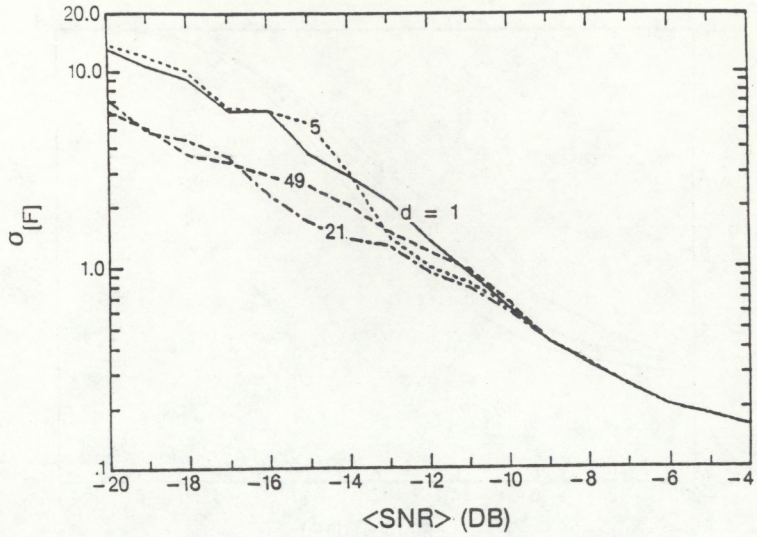

Figure 23. Standard deviation of consensus average [F] as a function of <SNR> for the same simulations as in Fig. 21.

7. SUMMARY

The simulations demonstrate that the smoothed finders yield better accuracy in the mean frequency estimate than the simple peak finder when <SNR> is marginal. The best results occur when σ_s of the smoothing function and $\langle\sigma\rangle$ of the signal spectrum are approximately equal. This match is not critical, for a difference of a factor of two in either direction between σ_s and $\langle\sigma\rangle$ is still superior to the peak finder. However, if the signal energy is concentrated in one spectral point, the peak finder is preferred. The slope of σ_F versus <SNR> steepens where the noise begins to interfere with locating the Doppler signal. The smoothed finder shifts this change in slope to lower <SNR>.

Once the peak of the smoothed spectrum is located at i_p, a subsearch on the unfiltered spectrum must select a spectral point if, where the signal exceeds the noise level. A subsearch for the nearest point above the noise level was slightly superior to a subsearch for the peak over the span d centered on i_p.

The rectangular and cosine-squared filters gave similar results, although the latter was somewhat more stable when σ_s far exceeds $\langle\sigma\rangle$. Sensitivity studies were performed with the cosine-squared smoother (Method 4), because it performed the best overall.

The sensitivity studies show that an exact match between the shape of the spectrum and the smoother is of secondary importance for unimodal spectra. As <σ> increases, the benefit from the best smoother changes from a large magnitude over a limited <SNR> range to lesser magnitudes over a wider <SNR> range. The smoothers also yield more improvement in the accuracy of F when the number of spectral points (or Nyquist frequency) increases while <σ> remains constant. As the number of spectra in the average increases, the degree of improvement increases slightly. A comparison of Figs. 11 and 15 shows that the advantage of the smoother is not purely a function of <σ>/K, but for constant <σ>/K the smoother provides greater advantage when K is larger.

The improvement for weak signal detection was also evaluated in terms of the amount of decrease in <SNR> that a smoother made possible with no loss in overall accuracy for F. The best choice of d typically achieves an allowable decrease of slightly more than 2 dB, although this depends somewhat on the situation. This alteration of effective sensitivity applies only in the weak signal regime, because the finders converge to identical performance as <SNR> increases. An improvement in effective sensitivity could help fill gaps that sometimes appear in profiler data. The superior signal processing might also allow a relaxation of hardware specifications with no overall loss of accuracy.

The improvements in accuracy or effective sensitivity also carry through the consensus averaging process. Simulations show that the consensus succeeds more frequently in marginal <SNR> when the individual values of F are found with a smoothed finder. The accuracy of this higher proportion of consensus averages is also better than with peak detection.

8. REFERENCES

Berger, T., and H.L. Groginsky, 1973: Estimates of the spectral moments of pulse trains. Proceedings, International Conf. on Information Theory, Tel-Aviv, Israel.

Chadwick, R.B., and N. Hassel, 1987: Profiler: the next generation surface-based atmospheric sounding system. Preprints, Third Int. Conf. on Interactive Information and Processing Systems for Meteorology, Oceanography, and Hydrology. January 12-16, 1987, New Orleans, Louisianna, Amer. Meteor. Soc., Boston, 15-21.

Hildebrand, P.H., and R.S. Sekhon, 1974: Objective determination of the noise level in Doppler spectra. J. Appl. Meteor., 13, 808-811.

Sirmans, D., and B. Bumgarner, 1975: Numerical comparison of five mean frequency estimators. J. Appl. Meteor., 14, 991-1003.

Strauch, R.G., K.B. Earnshaw, D.A. Merritt, K.P. Moran, and D.W. van de Kamp, 1984a: Performance of the Colorado wind-profiling network. Middle Atmosphere Program; Handbook for MAP, vol. 14, URSI/SCOSTEP Workshop on Technical Aspects of MST Radars, May 22-25, 1984. (Available from SCOSTEP Secretariat, Univ. of Illinois, 1406 W. Green St., Urbana, IL (61801) 38-48.

Strauch, R.G., D.A. Merritt, K.P. Moran, K.B. Earnshaw and D. van de Kamp, 1984b: The Colorado wind-profiling network.

Zrnic, D.S., 1975: Simulation of weatherlike Doppler spectra and signals. J. Appl. Meteor., 14, 619-620.